

Collective superlubricity of graphene flakes

Merel M. van Wijk,¹ Astrid S. de Wijn,² and Annalisa Fasolino¹

¹*Radboud University, Institute for Molecules and Materials,
Heyendaalseweg 135, 6525 AJ Nijmegen, The Netherlands*

²*Department of Physics, Stockholm University, 106 91 Stockholm, Sweden*

We investigate solid lubrication of graphene and graphene flakes using atomistic molecular-dynamics simulations. We find that graphene flakes yield lower friction than graphene as a result of a collective mechanism that emerges from the independent behaviour of the flakes. By freezing out different degrees of freedom of the flakes, we are able to attribute the low friction to non-simultaneous slipping of the individual flakes. We also compare the results of the atomistic simulations to those of a simplified two-dimensional model and find that the behaviour of the latter is strongly dependent on parameters, which emerge naturally from the atomistic simulations.

PACS numbers: 46.55.+d, 81.40.Pq, 62.20.Qp, 81.05.uf

INTRODUCTION

Graphitic systems are prototype systems for friction, particularly in the context of solid lubrication with layered materials. Moreover, since the discovery of graphene, there have been rapid developments of synthesis methods for other new two-dimensional materials, such as MoS₂, WS₂ or h-BN [1–3]. Wear of such lamellar materials results often in the formation of flakes [4–6]. In the last years, the notion that graphene and other layered materials are important for lubrication has led to much interest in this topic beyond the engineering community [7, 8]. One relevant question is whether large graphene layers are a better solid lubricant than nanoflakes.

Low friction due to structural incompatibility, dubbed structural superlubricity, was first observed in a graphene flake attached to an AFM tip sliding over a graphite substrate [9]. When the contact of the flake relative to the substrate was incommensurate a substantial reduction in friction was observed. Superlubric sliding over tens of nanometers was observed for graphene nanoflakes for temperatures as low as 5 K [10]. However, superlubric sliding is a fragile state, as flakes rotate back to the commensurate orientation [11, 12]. Mesoscopic flakes have been observed to retract to their original commensurate positions, after having been pushed away from equilibrium to an incommensurate angle [13].

Usually particles between sliding contacts, often called third bodies, increase the friction by pinning both sides of the contact [14–16]. Due to their flat and rather inert structure, graphene flakes might instead facilitate sliding. Some of the authors have previously examined whether graphene flakes could reduce friction between sliding graphite plates [17]. The model considered in that work represented an idealized situation with rigid flakes where out-of-plane motion, vibration and interactions between the flakes were neglected. That paper suggested a strategy to reduce friction by having one of the sliding surfaces made of graphene with patches with different

orientations formed e.g. by grain boundaries, in order to avoid that the flakes would be commensurate with both plates at any time. Although we believe this strategy beneficial, it is relatively cumbersome to realize in practical devices.

Here we examine a more realistic model based on an atomistic description of sliding graphite plates lubricated either by flakes or by a full graphene layer. We find that graphene flakes yield a state of low friction as a result of a collective mechanism emerging from independent behaviour. The crucial ingredient of this mechanism is that the flakes do not slip simultaneously. In the atomistic description, which naturally restricts the parameters to realistic values, this mechanism appears to be robust. The simple model of Ref. [17] might also show this type of behaviour but it is too sensitive to the precise choice of parameters to be predictive quantitatively.

SIMULATION SETUP

We construct a model of two graphene layers with between them either another graphene layer or n hexagonal flakes of N carbon atoms, terminated with hydrogen atoms. Unless stated otherwise, each graphene layer measures $77.5\text{\AA} \times 83.9\text{\AA}$ (2560 atoms), $N = 24$ and $n = 29$. The latter values result in a ratio of $\rho = 0.27$ between the number of carbon atoms in the flakes and those in a graphene layer. The system is shown in Fig. 1. The bottom layer is immobile while the top layer is fully mobile and pulled in the x -direction at a velocity $v = 10$ m/s by springs with spring constant $K = 1$ meV/ \AA^2 , attached to every atom. In the appendix we discuss this choice and the effect of weaker and stronger K .

The sum of the force on all springs yields the lateral force F_x . Assuming an area A of the graphene layer as above, $F_x = 1$ eV/ \AA = 1.6 nN gives a stress $\tau = F_x/A = 2.464 \cdot 10^7$ Pa. The resulting friction is calculated as the average of F_x over a few periods of the motion. We performed molecular dynamics simulations

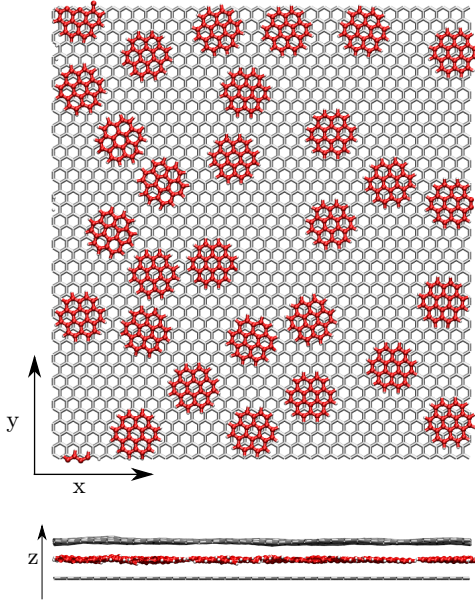


FIG. 1: Top view and side view of our model.

for up to 10 periods, using the molecular dynamics code LAMMPS [18].

The moving top layer is thermostatted by a Langevin thermostat with damping constant $\gamma = 1$ ps at $T = 300$ K. The flakes are not directly thermostatted to avoid complications with thermostating of rigid flakes and treating fully mobile and rigid flakes differently.

The interactions within one layer are given by the REBO potential [19] as implemented in LAMMPS, while the interlayer interactions are given by the Kolmogorov-Crespi potential [20]. The equilibrium bond length d of the intralayer REBO potential in lammps is 1.3978 Å, yielding a period $a = \sqrt{3}d = 2.42$ Å, slightly smaller than the experimental value. Therefore we rescale the Kolmogorov-Crespi potential to this value. Also, we do not include bending terms in the Kolmogorov-Crespi potential as our layers are flat compared to the nanotubes for which the potential was developed. We have also considered geometries with more layers and different schemes for thermostating (see Appendix).

FRICION AND SLIPPAGE

Fig. 2 shows that a much lower friction is found when flakes instead of a full layer are placed between the graphite plates. With a full layer, the lateral force displays a distinctive stick-slip high-friction behaviour whereas the flakes lead to a smoother behaviour with broader downward profile, resulting in lower friction. For the layer, after the first three periods the centre of mass displays a very regular motion, jumping from one mini-

mum to the next. The dynamics of the flakes is instead much more complex as we will describe later. The difference in the friction cannot be explained by the lower coverage, which leads to a lower potential energy barrier against sliding but cannot account for the reduction of more than a factor 5 shown in Fig. 2.

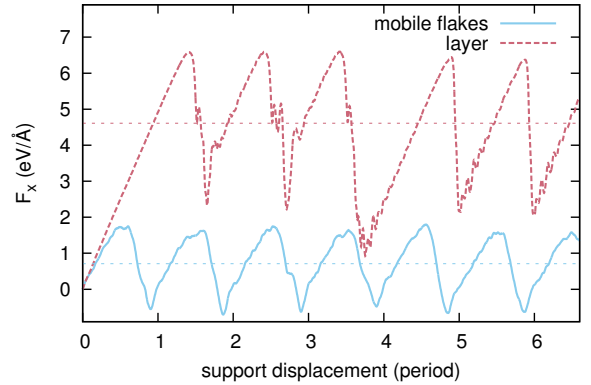


FIG. 2: Lateral force as a function of support displacement for contacts with either graphene flakes or a graphene layer. The friction is lower for the case with flakes. In addition, the lateral force with flakes does not have the standard saw-tooth profile resulting from stick-slip motion that the force for a graphene layer does display.

In order to elucidate the mechanism for the reduction of the friction, we have investigated several cases where different degrees of freedom of the flakes were frozen. We first consider flakes that are rigid, but otherwise free to translate and rotate, and also entirely immobile flakes that are fixed to the bottom substrate in commensurate orientation. In Fig. 3 we show the results of these simulations in comparison with the fully mobile flakes. In the case with immobile flakes attached to the substrate, friction is still considerably lower than for a full layer due to the lower coverage, but the lateral force clearly shows stick-slip behaviour. The friction for mobile and rigid flakes is much lower than for the fixed flakes and with a less pronounced stick-slip character. The internal degrees of freedom of the mobile flakes lower the friction only marginally. Very small differences in friction are also found when comparing fully mobile flakes to flakes restricted to move only in the in-plane direction (not shown).

One might think that rotations of the flakes away from commensurate contacts are crucial for the low friction state. Surprisingly, we have found instead that we can also eliminate rotations of the flakes as the main cause of the low friction. In Fig. 4. we compare situations with restricted types of motion. The lateral force for rigid flakes that cannot rotate (translation only) is very similar to that of rigid flakes that can both rotate and translate (rigid). This comparison excludes rotations as origin of the low friction. In contrast, not allowing translational

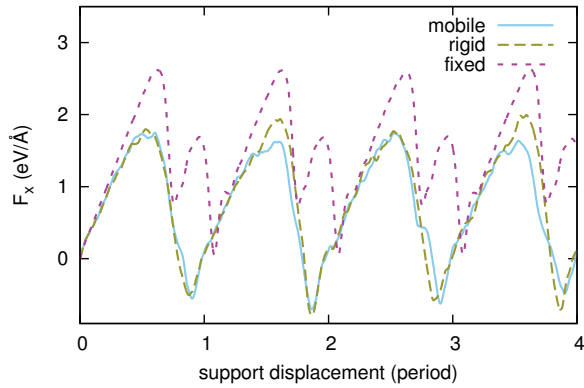


FIG. 3: Lateral force as a function of support displacement (time) for different cases: (i) fixed flakes, (ii) rigid flakes, (iii) fully mobile flakes. Both the fully mobile and rigid flakes have lower friction and do not show the distinctive stick-slip shape.

motion (rotation only) leads to a much higher friction and stick-slip behaviour. We have also examined the range of rotations occurring during the motion. In Fig. 5 we see that freezing of degrees of freedom leads to a higher probability of commensurate contact, as signaled by a sharper peak at zero degrees.

Having eliminated internal vibrations and rotations of the flakes as main reason of the lower friction, we show next that the crucial ingredient is that the flakes move independently. This conclusion can be drawn by examining the dynamics obtained by averaging the force on the flakes, i.e. by making the flakes move as one body. The corresponding lateral force (labeled one-body in Fig. 4) displays stick-slip and high friction. The friction is similar to the case of immobile flakes (Fig. 3) and flakes that can only rotate (Fig. 4), although the static friction, i.e. the height of the lateral force peaks, is lower.

The cause of lower friction then, can be found in the non-simultaneous collective translations of the flakes. We characterize their translational dynamics in Fig. 6, where we show the x-position of the centre of mass of the individual flakes as a function of time. When the flakes are stuck, they move on average with half the sliding velocity, that is, with the average velocity of top and bottom layer. One can also see the rapid movement of the flakes when they slip, but also that these slips do not occur simultaneously for all flakes so that it is not possible to recognize the period of the motion in Fig. 6. Rather than moving all at once, which would result in a single large slip of the top graphene sheet, there is continuous slippage of flakes one by one. This leads to the smoother force profile shown in Fig. 2 but, as there is still stick-slip occurring on smaller scales, the force still displays some of the typical characteristics of stick-slip, such as temporary negative lateral forces. When the flakes are rigid (Fig. 6b), the slips are longer. This is to be expected, as internal degrees of freedom are expected to dampen

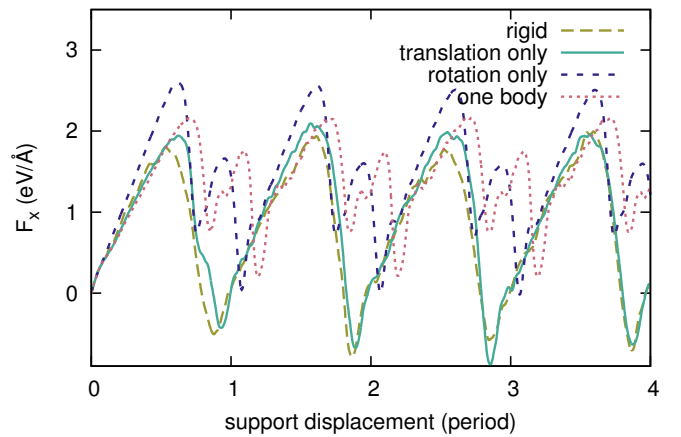


FIG. 4: Lateral force as a function of support position (time) for rigid flakes with either total force on each flake set to zero, enabling only rotations, or the torque on each flake set to zero, enabling only translations, or the rigid flakes where both translations and rotations are allowed. The friction curve with only rotations closely resembles that of fixed flakes, while the translations only is close to the one of the rigid flakes. The line labeled ‘one body’ has the force on the flakes averaged, thus enabling only translations of all flakes moving as one body. This resembles the case of fixed flakes, but with lower static friction.

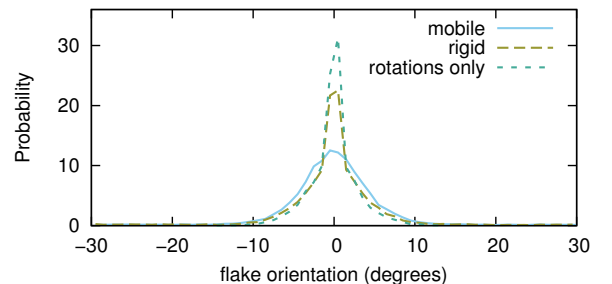


FIG. 5: Distribution of angles for mobile flakes, rigid flakes and flakes where where the force is set to zero (rotations only).

the movement. The effect on the lateral force is however negligible as shown in Fig. 3.

In Fig. 7, we show the distribution of slips throughout one lattice period of the support motion. A slip has been defined as the motion of a flake for more than one quarter of the lattice period relative to the fixed bottom plate during a time interval of 0.5 ps. One can see that slips occur during all phases of the period.

In the Appendix, we also include a brief comparison to the simple two-dimensional model of Ref. 17, which has rigid plates, rigid flakes, and a sinusoidal interaction potential. In such simple models, the choice of parameters is a challenge as they have to be estimated indirectly. As shown in the Appendix, the behaviour of the model may depend strongly on the choice of parameters. Atomistic descriptions present an advantage in this respect, as

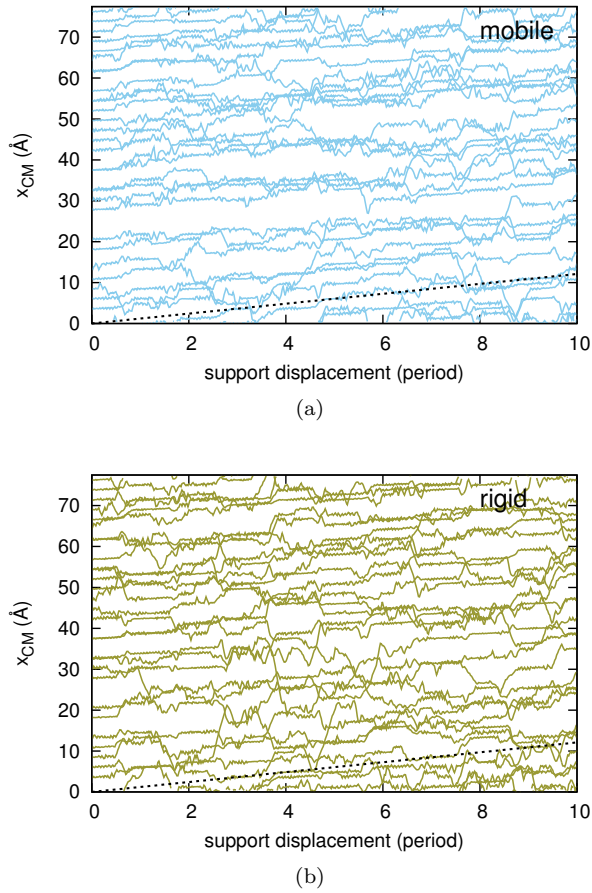


FIG. 6: Position along the x-axis of the flakes as a function of time (expressed in terms of support displacement) for a) fully mobile flakes, b) rigid flakes. The flakes themselves perform stick-slip motion, but do not slip simultaneously. Moreover, they sometimes stick to the graphene sheet above them and sometimes to the one below. During a stick, the flakes stick to both plates and so move with half the support velocity (indicated by the black line).

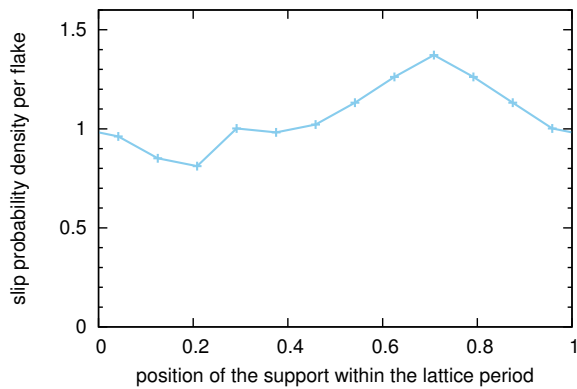


FIG. 7: The distribution of slips of single flakes during the time needed for the support to move by one period of the lattice. Slips were detected as a change of position in the sliding direction of more than $1/4$ lattice period during 0.5 ps. Slips typically occur over half a lattice period, due to the hexagonal lattice.

realistic parameter values emerge naturally.

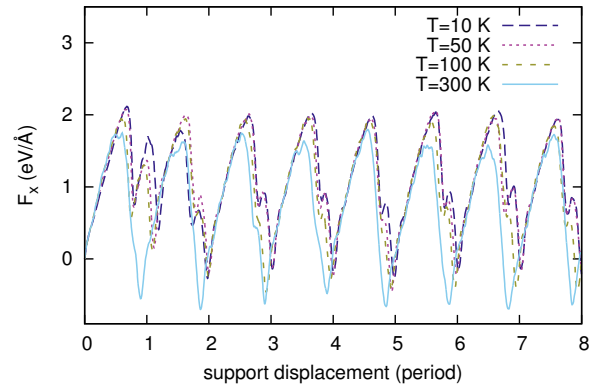


FIG. 8: Lateral force as a function of support position for different temperatures. The friction is higher and tends more towards stick-slip for lower temperatures.

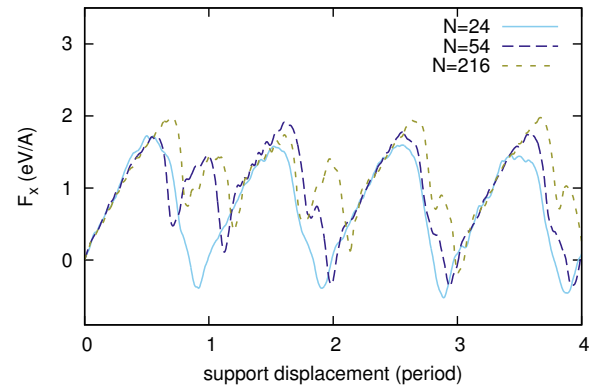


FIG. 9: Lateral force as a function of support position for H-saturated hexagonal flakes of different size. We consider 27 flakes of 24 carbon atoms, 12 flakes of 54 atoms and 3 flakes of 216 atoms. Each graphite plate measures $77.5\text{Å} \times 75.4812\text{Å}$ and the total number of flake atoms is equal to keep $\rho = 0.28$.

Finally, we include several numerical results from the atomistic simulations that explore the effects of other parameters, namely temperature and flake size. In Fig. 8, the lateral force is plotted for several different temperatures. As usual, due to thermal activation of slips, for higher temperatures the friction is lower [21]. Figure 9 shows the lateral force for a number of different flake sizes, with the same total number of atoms in the flakes. For larger flakes, the friction is higher. This is to be expected as larger flakes interact more strongly with the substrate and are less subject to thermal fluctuations. As a result, the larger flakes slip more simultaneously than the smaller ones.

CONCLUSIONS

By means of realistic molecular dynamics simulations, we have shown that graphene flakes reduce the friction when compared to a perfect graphene layer. This is not only due to the lower coverage which reduces the potential energy barrier, but also to the fact that there are many independently moving flakes. The flakes slip at different times within one period, causing the top layer to slide more smoothly. The independent collective behaviour of the flakes is a way of lowering friction not studied before.

By freezing out degrees of freedom we have examined the effects of different contributions to the movement of the flakes on the friction separately, making it possible to rule out the role of internal vibrations and rotations of the flake as a determining factor for the low friction behaviour. Our results suggest that graphene nanoflakes are more suitable for coatings than perfect graphene layers for low friction devices.

Acknowledgements We thank Michael Urbakh (Tel Aviv), Staffan Jacobson, Krisztina Kadas, Jill Sundberg and Harald Nyberg (Uppsala) for interesting discussions. M.M.v.W and A.F. acknowledge support of the Foundation for Fundamental Research on Matter (FOM), which is part of the Netherlands Organisation for Scientific Research (NWO) within the program n.129 “Fundamental Aspects of Friction”. A.S.d.W.’s work is financially supported by an Unga Forskare grant from the Swedish Research Council. This work is supported in part by COST Action MP1303.

APPENDIX

Comparison to the simple model of Ref. [17]

Here, we also include a brief comparison to the simple two-dimensional model of Ref. 17. This model is similar in setup to the atomistic description in the current work. It consists of two rigid plates in two-dimensions, one of which is fixed, and the other is pulled by a spring connected to a support moving at constant velocity. A collection of rigid flakes is interacting with both plates through a sinusoidal potential.

We simulate the simple model with the parameters used in Ref. [17], with the exception of the pulling angle, which is set to 0 for reasons of clarity. We also consider several variations of the parameters. Figure 10 shows force traces for the simple model with the original parameters, as well as results of a simulation with similar, but slightly modified parameter values. It is clear that the behaviour of the simple model depends dramatically on the parameter values. The force traces show different slip lengths, as well as transitions between stick-slip and

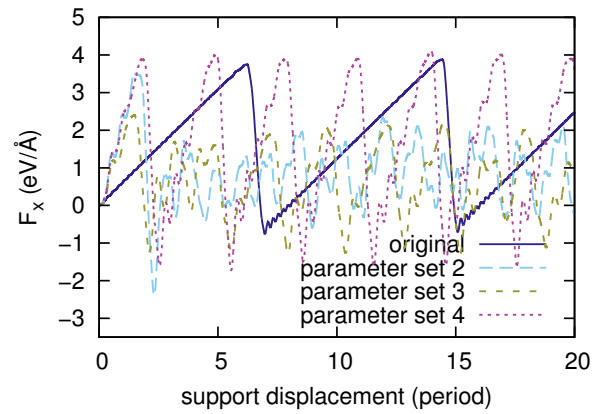


FIG. 10: Lateral force as a function of support position for the simple model from Ref. [17] for several parameter sets. “Original” refers to the parameters used in Ref. [17]. “Parameter set 2” refers to very similar parameters but with both the tip spring constant and the tip mass multiplied by a factor of 4. “Parameter set 3” refers to the same parameters as “Parameter set 2”, except that also the damping parameter is multiplied by a factor of 4. Finally, “Parameter set 4” refers to the same parameters as “Parameter set 3”, but with the temperature and sliding speed adjusted to match the current atomistic description. For each of these sets of parameters the model behaves radically differently. Nevertheless, between the different simulations only very few parameters are different, and they differ by less than an order of magnitude.

more smooth-sliding like behaviour, or even irregular dynamics. Nevertheless, between the different simulations only very few parameters are different, and they differ by less than an order of magnitude. Without an accurate atomistic description, it is difficult to know which of these parameter values most accurately describe a realistic system.

In previous work on the simple model, the tip mass was taken to be equal to the mass of the flakes, whereas in the more realistic atomistic description, it is almost four times larger. Similarly, the spring constant, which was taken to be similar to the spring constant of an AFM tip with a sharp apex, is an underestimate of the spring constant of a large, blunt piece of graphite. While these parameter values appear naturally in the atomistic description, they are not directly obvious for a simple model.

Effect of number of layers and thermostat

We performed simulations with a different number of layers and different thermostat settings. In Fig. 11 we show that smooth-like sliding with low friction occurs for all cases. Thermostatting the flakes (the line labeled “3L*” in Fig. 11) does not have much effect. When a graphene layer is added between the top layer and the flakes that is also thermostatting (4L*), the friction is slightly higher, probably due to the increased damping

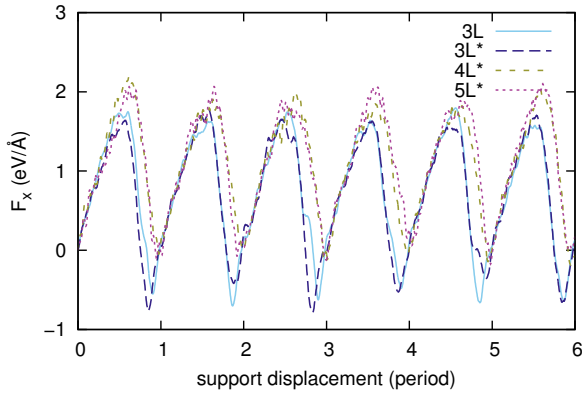


FIG. 11: This shows lateral force curves for different number of layers. “3L” refers to the situation as in the main text. “3L*”, “4L*”, “5L*” refers to a system with 3 layers, 4 layers, 5 layers respectively with a thermostat on all mobile atoms.

(lowering the damping constant also results in the addition of a constant value to the lateral force). This is also true when another layer is added between the flakes and the bottom layer (5L*).

Effect of spring constant

The choice of K is always a delicate point in simulations of friction because it depends on the theoretical model or experimental setup. In Fig. we compare the lateral force presented in the main text for a full layer with $K = 1 \text{ meV}/\text{\AA}^2$ to those with a fivefold stronger or weaker K . One can see that smaller K gives an irregular behaviour with long jumps whereas a stiffer K leads to strong oscillations with the current, standard, choice of the damping parameter of 1 picosecond.

The value $K = 1 \text{ meV}/\text{\AA}^2$ we use is consistent with the elastic effects of a block of material with the size of our cell, a height of 16 \AA and the typical Young’s modulus of graphite, 10 GPa . Notice that usually the Tomlinson model is implemented by means of a total spring constant attached to the center of mass, whereas we report the spring constant per atom with periodic boundary conditions. The chosen spring constant per atom $K = 1 \text{ meV}/\text{\AA}^2$ is equal to 0.016 N/m per atom, which brings the total spring constant in our 2560 atom system to 40.96 N/m . Note also that we do not impose any load, and the effects of a weaker spring constant are similar to keeping the same spring constant while imposing a load.

- [3] A. K. Geim and I. V. Grigorieva, *Nature* **499**, 419 (2013).
- [4] L. Rapoport, N. Fleischer, and R. Tenne, *Advanced Materials* **15**, 651 (2003).
- [5] J. M. Martin, C. Donnet, T. Le Mogne, and T. Epicier, *Phys. Rev. B* **48**, 10583(R) (1993).
- [6] L. Joly-Pottuz, F. Dassenoy, M. Belin, B. Vacher, J. M. Martin, and N. Fleischer, *Tribology letters* **18**, 477 (2005).
- [7] D. Berman, A. Erdemir, and A. V. Sumant, *Materials Today* **17**, 31 (2014).
- [8] K.-S. Kim, H.-J. Lee, C. Lee, S.-K. Lee, H. Jang, J.-H. Ahn, J.-H. Kim, and H.-J. Lee, *ACS nano* **5**, 5107 (2011).
- [9] M. Dienwiebel, G. S. Verhoeven, N. Pradeep, J. W. M. Frenken, J. A. Heimberg, and H. W. Zandbergen, *Phys. Rev. Lett.* **92**, 126101 (2004).
- [10] X. Feng, S. Kwon, J. Y. Park, and M. Salmeron, *ACS Nano* **7**, 1718 (2013).
- [11] A. E. Filippov, M. Dienwiebel, J. W. M. Frenken, J. Klafter, and M. Urbakh, *Phys. Rev. Lett.* **100**, 046102 (2008).
- [12] A. S. de Wijn, C. Fusco, and A. Fasolino, *Phys. Rev. E* **81**, 046105 (2010).
- [13] Z. Liu, J. Yang, F. Grey, J. Z. Liu, Y. Liu, Y. Wang, Y. Yang, Y. Cheng, and Q. Zheng, *Phys. Rev. Lett.* **108**, 205503 (2012).
- [14] I. L. Singer, *MRS bull.* **23**, 37 (1998).
- [15] G. He, M. H. Müser, and M. O. Robbins, *Science* **284**, 1650 (1999).
- [16] M. H. Müser, L. Wenning, and M. O. Robbins, *Physical Review Letters* **86**, 1295 (2001).
- [17] A. S. de Wijn, A. Fasolino, A. E. Filippov, and M. Urbakh, *Europhysics Lett.* **95**, 66002 (2011).
- [18] S. Plimpton, *J. Comput. Phys.* **117**, 1 (1995).
- [19] D. W. Brenner, O. A. Shenderova, J. A. Harrison, S. J. Stuart, B. Ni, and S. B. Sinnott, *J. Phys.: Condens. Matter* **14**, 783 (2002).
- [20] A. N. Kolmogorov and V. H. Crespi, *Phys. Rev. B* **71**, 235415 (2005).
- [21] K. B. Jinesh, S. Y. Krylov, H. Valk, M. Dienwiebel, and J. W. M. Frenken, *Phys. Rev. B* **78**, 155440 (2008).

-
- [1] H. Nyberg, J. Sundberg, E. Särhammar, T. Nyberg, U. Jansson, and S. Jacobson, *Tribol. Lett.* **56**, 563 (2014).
 - [2] F. Gustavsson, S. Jacobson, A. Cavaleiro, and T. Polcar, *Surf. & Coat. Tech.* **232**, 541 (2013).